JOURNAL OF MARINE RESEARCH

The *Journal of Marine Research,* one of the oldest journals in American marine science, published important peer-reviewed original research on a broad array of topics in physical, biological, and chemical oceanography vital to the academic oceanographic community in the long and rich tradition of the Sears Foundation for Marine Research at Yale University.

An archive of all issues from 1937 to 2021 (Volume 1–79) are available through EliScholar, a digital platform for scholarly publishing provided by Yale University Library at https://elischolar.library.yale.edu/.

Requests for permission to clear rights for use of this content should be directed to the authors, their estates, or other representatives. The *Journal of Marine Research* has no contact information beyond the affiliations listed in the published articles. We ask that you provide attribution to the *Journal of Marine Research.*

Yale University provides access to these materials for educational and research purposes only. Copyright or other proprietary rights to content contained in this document may be held by individuals or entities other than, or in addition to, Yale University. You are solely responsible for determining the ownership of the copyright, and for obtaining permission for your intended use. Yale University makes no warranty that your distribution, reproduction, or other use of these materials will not infringe the rights of third parties.

Plankton community composition, organic carbon and thorium-234 particle size distributions, and particle export in the Sargasso Sea

by H. S. Brew[1], S. B. Moran[1,2], M. W. Lomas[3] and A. B. Burd[4]

ABSTRACT

Measurements of plankton community composition (eight planktonic groups), particle size-fractionated (10, 20, 53, 70, and 100-μm Nitex screens) distributions of organic carbon (OC) and ^{234}Th, and particle export of OC and ^{234}Th are reported over a seasonal cycle (2006–2007) from the Bermuda Atlantic Time-Series (BATS) site. Results indicate a convergence of the particle size distributions of OC and ^{234}Th during the winter-spring bloom period (January–March, 2007). The observed convergence of these particle size distributions is directly correlated to the depth-integrated abundance of autotrophic pico-eukaryotes (r = 0.97, P < 0.05) and, to a lesser extent, *Synechococcus* (r = 0.85, P = 0.14). In addition, there are positive correlations between the sediment trap flux of OC and ^{234}Th at 150 m and the depth-integrated abundance of pico-eukaryotes (r = 0.94, P = 0.06 for OC, and r = 0.98, P < 0.05 for ^{234}Th) and *Synechococcus* (r = 0.95, P = 0.05 for OC, and r = 0.94, P = 0.06 for ^{234}Th). An implication of these observations and recent modeling studies (Richardson and Jackson, 2007) is that, although small in size, pico-plankton may influence large particle export from the surface waters of the subtropical Atlantic.

1. Introduction

Plankton community composition is a fundamentally important determinant of both the magnitude and mechanisms of particulate organic carbon (POC) export from the upper-ocean (Boyd *et al.,* 1999; Kawakami and Honda, 2007; Lomas and Bates, 2004; Wassmann, 1998). In oligotrophic regions, the classic paradigm is that large, rapidly sinking cells contribute disproportionately to export as compared to small cells (Michaels and Silver, 1988). In the traditional model, pico-sized (<3-μm) organisms are responsible for most of the open-ocean's primary production and are retained in the euphotic zone via the microbial loop. However, despite their small size, pico-plankton are increasingly recognized for their dynamic role in open-ocean carbon cycle processes. Recent evidence suggests that aggregates of pico-plankton may contribute significantly to the downward

1. Graduate School of Oceanography, University of Rhode Island, Narragansett, Rhode Island, 02882, U.S.A.
2. Corresponding author. ***email: moran@gso.uri.edu***
3. Bermuda Institute of Ocean Sciences, St. Georges, Bermuda GE01.
4. Department of Marine Sciences, University of Georgia, Athens, Georgia, 30602, U.S.A.

sinking flux of organic carbon (OC) in direct proportion to their abundance in the euphotic zone (Olli *et al.,* 2002; Richardson and Jackson, 2007).

Plankton community structure may differentially affect POC fluxes determined using sediment traps and ^{234}Th/^{238}U disequilibria, which are the primary techniques used to quantify the rate of upper ocean POC export. In this regard, laboratory (Quigley *et al.,* 2002) and field (Guo *et al.,* 2002; Hung *et al.,* 2004; Santschi *et al.,* 2003) studies demonstrate that acid polysaccharide exudates from different plankton species can significantly influence the POC/^{234}Th ratio of marine particles, which is important because the POC/^{234}Th ratio is a key parameter in quantifying POC export using ^{234}Th/^{238}U disequilibria (Moran *et al.,* 2003; Smith *et al.,* 2006). Moreover, free-floating, surface-tethered sediment traps may ineffectively capture the small, slowly sinking component of the particle flux due to hydrodynamic "winnowing" (Gustafsson *et al.,* 2004; Buesseler *et al.,* 2007). There have also been laboratory studies of phytoplankton-radiotracer interactions (e.g., Fisher *et al.,* 1987) and field measurements of ^{234}Th and selected pigments (e.g., Baskaran *et al.,* 1996); however, few field studies have reported simultaneous measurements of POC export, ^{234}Th/^{238}U disequilibria, POC/^{234}Th ratios, and plankton community structure.

In an effort to better define the relationship between plankton community composition and export, this study reports contemporaneous measurements of plankton community composition and particle size distributions and fluxes of OC and ^{234}Th over a seasonal cycle at the Bermuda Atlantic Time-Series (BATS) site.

2. Methods

a. Sample collection and at-sea processing

Samples were collected at the Bermuda Atlantic Time Series (BATS) site (31°40′N, 64°10′W) aboard the R/V *Atlantic Explorer* on four cruises between May 2006 and March 2007 (Steinberg *et al.,* 2001). Primary productivity, sediment trap POC export, phototrophic pico- and nano-plankton cell enumeration, temperature, salinity, and fluorescence data were collected as part of the BATS sampling regimen (DuRand *et al.,* 2001; Steinberg *et al.,* 2001).

During three of the cruises (November, 2006, January, 2007, March, 2007), ~80 L of water was collected from 4–5 of the *in-situ* pump depths and filtered (0.08–0.45 L min^{-1}) through three 25-mm diameter in-line filter holders connected in series and fitted with Nitex screens (53, 70, and 100-μm). After ~10–80 L passed through the filter series, the screens were removed, fixed with alkaline Lugol's solution (1% Lugol's iodine and sodium acetate) and mounted onto glass slides for microscopic examination.

A drifting sediment trap array with cylindrical traps (collection area 0.0039 m^2) suspended at 150, 200 and 300 m was deployed for 1.8–4.3 days during each sampling period (Table 1). Sediment traps were prepared and processed according to the BATS sampling protocol, including picking swimmers from each tube prior to POC and ^{234}Th analysis (Steinberg *et al.,* 2001). Two traps at each depth were treated as replicates for either POC or ^{234}Th determination.

Table 1. Samples collected on BATS cruises between May 2006 and March 2007.

BATS ID	Dates	Collection method	Depth range (m)
B211	May 9–12, 2006	*In-situ* Pump [234]Th and POC	100–500
		SV [234]Th	10–500
		Trap deployment 3.1 d	150–300
		FCM	0–250
B217	Nov 6–11, 2006	*In-situ* Pump [234]Th and POC	75–500
		SV [234]Th	10–500
		Trap deployment 4.3 d	150–300
		FCM	0–250
		80 L plankton filtration Microscopic enumeration	75–500
B219	Jan 27–Feb 2, 2007	*In-situ* Pump [234]Th and POC	75–500
		SV [234]Th	10–500
		Trap deployment 1.8 d	150–300
		FCM	0–250
		80 L plankton filtration Microscopic enumeration	75–300
B221	Mar 19–24, 2007	*In-situ* Pump [234]Th and POC	75–500
		SV [234]Th	10–500
		Trap deployment 2.5 d	150–300
		FCM	0–250
		80 L plankton filtration Microscopic enumeration	75–500

In-situ Pump [234]Th and POC data are size fractionated particles ranging from $<$1–100-μm and 10–100-μm, respectively.

Dissolved [234]Th and particle size fractionated organic C and [234]Th were collected at 5–6 depths (Table 1) in the upper 500 m using large-volume *in-situ* pumps (Challenger Oceanic Systems and Services, Surrey, U.K., and McLane Laboratories, Falmouth, MA). Seawater (200–1000 L) was sequentially pumped through a series of three 142 mm diameter Nitex screens (for each depth; 10, 20, 53-μm on one cast; 53, 70, 100-μm on a second cast), a 1-μm cartridge filter (providing for each depth; 1–10 μm on one cast; 1–53 μm on the second cast), and two MnO_2-impregnated cartridges connected in series to scavenge dissolved [234]Th. Size fractionated particles collected on the Nitex screens were resuspended into GF/F filtered seawater with an ultrasonicator for five minutes, vacuum-filtered onto pre-combusted 25 mm Whatman GF/F filters (0.7-μm nominal pore size), and then stored frozen in Petri dishes until POC and [234]Th analysis.

Samples (4 L) were collected from 12 depths using the CTD rosette for small-volume (SV) [234]Th analysis (Buesseler *et al.,* 2001). Two or three SV [234]Th profiles were

determined on each cruise (Table 1). One hour after the addition of 25 mL of 0.2 M $KMnO_4$, 10 mL of 1 M $MnCl_2$, and 7–8 drops of concentrated NH_4OH, samples were vacuum-filtered (~ 0.13 L min^{-1}) through 25 mm GM/F filters (1-μm nominal pore size) and stored in Petri dishes until ^{234}Th analysis.

b. Plankton community composition analysis

The relative abundance of organisms retained on the 25 mm diameter Nitex screens (53, 70, and 100-μm) was determined through microscopic examination. Particles retained on these Nitex screens (mounted on microscope slides as described above), were categorized and enumerated using a Nikon (model S-Ke, coaxial focusing) light microscope in bright-field mode at 100X magnification. Based on prior experience, an estimated counting error of 10% was applied to all count data.

All identifiable organisms were enumerated on each screen. The taxonomic groups included in this study were zooplankton, radiolaria, dinoflagellates, and diatoms. These groups were chosen as they could be identified with the highest degree of confidence. Although other organisms were present, limitations of the experimental design did not allow for their inclusion in this study.

Water column (0–250 m) cell abundances of cyanobacteria (*Prochlorococcus* and *Synechococcus*), and autotrophic pico- and nano-eukaryote cells were determined on a high sensitivity Cytopeia Influx Flow Cytometer (FCM). Samples were fixed in para-formaldehyde (0.5% final concentration) and stored at $-80°$C prior to laboratory analysis. Prior to enumeration, cells were categorized using two-dimensional scatter plots (DuRand and Olson, 1996). Pico-cyanobacteria were identified as *Prochlorococcus* or *Synechococcus* based upon cell size and the absence or presence of the pigment phycoerythrin. Chlorophyll containing auto-fluorescent cells ~ 1 to 3-μm and >3-μm were identified as pico-eukaryotes and nano-eukaryotes, respectively (DuRand and Olson, 1996; DuRand *et al.,* 2001). Cells in each category were enumerated and the results converted to cell abundance using the method of Sieracki *et al.* (1993), with estimated counting uncertainties of $\sim \pm 2$–3% at cell abundances >200 cells mL^{-1}.

c. ^{234}Th, ^{238}U and POC determination

The ^{234}Th activity of large-volume size fractionated particulate (142 mm diameter, 10, 20, 53, 70, and 100-μm Nitex), SV, and sediment trap samples was determined by beta emission of ^{234m}Pa ($E_{max} = 2.19$ MeV) using a RISØ National Laboratory low-background beta detector (Charette *et al.,* 2001). Samples were counted approximately once per week for three weeks during the first 50 days after sample collection and one additional time ~ 150 days after sample collection to determine background ^{234}Th. Count data were decay-corrected to the midpoint of sample collection by best-fit of the weekly count data. Large-volume particulate (10, 20, 53, 70, and 100-μm) subsamples and SV total ^{234}Th samples were mounted on acrylic disks and covered with one layer each of clear plastic (1.3 mg cm^{-2}) and aluminum foil (4.3 mg cm^{-2}) to decrease interference from low-energy

beta and alpha particle emitters. The ^{234}Th collection efficiency of the small-volume method was assumed to be 100%; this assumption is confirmed by the observation that the ^{234}Th/^{238}U activity ratio was ~1 in deep (500 m) waters. Sediment trap ^{234}Th was isolated through a series of anion-exchange columns using a ^{230}Th yield monitor (Buesseler *et al.,* 1992). The Th fraction was electroplated onto stainless steel disks and beta counted for ^{234}Th as described above.

Large-volume dissolved (<1-μm) and cartridge particulate (1–10-μm or 1–53-μm) ^{234}Th activities were determined by gamma spectrometry (Buesseler *et al.,* 1992). Cartridge filters (1-μm) and MnO$_2$-impregnated cartridges were dried at 50°C for approximately 24 hours and then combusted at 500°C overnight. The ash (3.5 g) was compacted to 4 mL in 10 mL polystyrene vials and counted at 63.3 KeV using a pure Ge well detector (detector efficiency 0.48 ± .01 for ^{234}Th in this sample geometry). The resulting count data were then decay-corrected to the midpoint of sample collection. Dissolved ^{234}Th activities (Th_d, dpm L^{-1}) were calculated after correction for the MnO$_2$ cartridge collection efficiency. Average collection efficiencies were 0.88 ($\sigma = 0.06$, $N = 11$) in May, 0.90 ($\sigma = 0.03$, $N = 12$) in November, 0.89 ($\sigma = 0.05$, $N = 6$) in January, and 0.87 ($\sigma = 0.10$, $N = 11$) in March. ^{238}U was determined at each station depth using the relationship ^{238}U $= 0.0708 \times$ salinity (dpm L^{-1}) (Chen *et al.,* 1986).

Subsamples of particulate (142 mm diameter, 10, 20, 53, 70, and 100-μm Nitex) material collected using *in-situ* pumps were cut (approximately 10% by weight) from 25 mm Whatman GF/F filters using ceramic scissors for POC analysis. POC samples were dried at 50°C overnight, acidified in fuming HCl in an acid dessicator for 24 hours, and dried (Pike and Moran, 1997). POC concentrations were measured using a CE 440 Elemental Analyzer (Exeter Analytical, Inc., Chelmsford, MA). The average POC blank of dry, pre-combusted GF/Fs was 4.80 μmol C ($N = 5$, $\sigma = 0.34$) and used for all sample blank corrections.

3. Results

a. Hydrography and primary production

Water column (0–200 m) temperature, chlorophyll concentration (L^{-1}), density anomaly, and integrated (0–140 m) primary production from April 2006 through April 2007 are illustrated in Figure 1 (http://bats.bios.edu). Surface temperature increased in May 2006 and water column stratification intensified throughout the summer and fall months. In December 2006 and January 2007, water column de-stratification began and continued throughout the remainder of the annual cycle. Seasonal maxima in chlorophyll *a* concentrations were observed throughout the euphotic zone from January to April 2007 during the winter/spring bloom, with only a deep chlorophyll maximum observed from May through December 2006, consistent with previous observations.

Integrated (0–140 m) primary production varied throughout the annual cycle (Fig. 1). Primary production increased by a factor of ~2 from January (76.1 mmol C m^{-2} d^{-1}) and
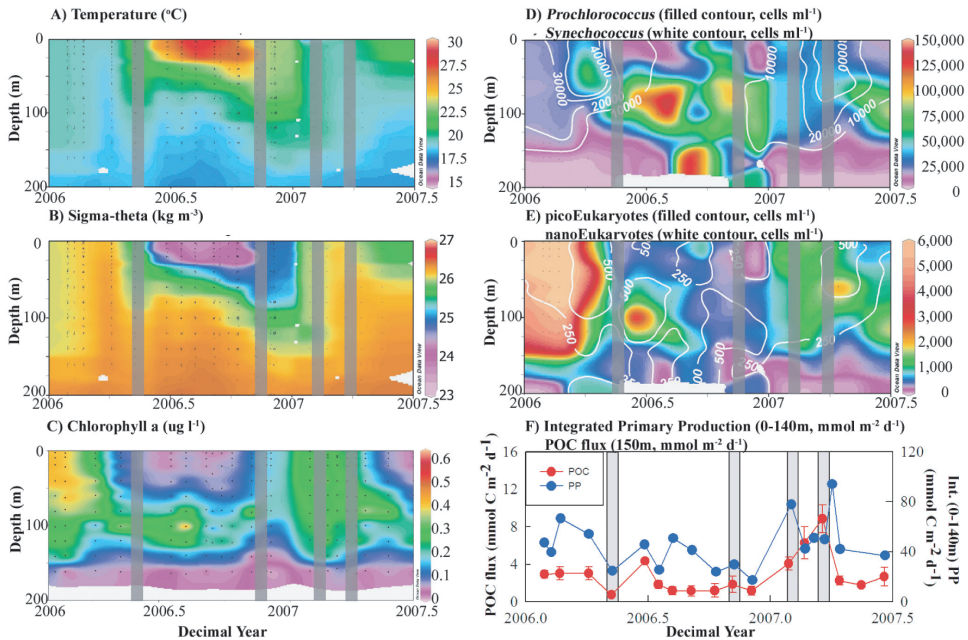
Figure 1. Upper ocean (0–200 m) temperature, sigma-theta, chlorophyll-*a,* cell concentrations of autotropic *Prochlorococcus, Synechococcus,* pico- and nano- eukaryotes, integrated (0–140 m) primary production, and POC export at 150 m at the BATS site from April 2006–April 2007. Shaded bars indicate the months sampled in this study.

March (50 mmol C m^{-2} d^{-1}), which together averaged 63.1 mmol C m^{-2} d^{-1}, compared to May (24.7 mmol C m^{-2} d^{-1}) and November (29.8 mmol C m^{-2} d^{-1}), which together averaged 27.3 mmol C m^{-2} d^{-1}. The increase in primary production and chlorophyll *a* suggests the occurrence of a winter-spring bloom between January and April 2007. Data from May and November are consistent with seasonally averaged summer-fall data from 1990–present. Primary production rates observed in January and March 2007, however, were among the highest values measured during the past two decades at BATS (data available at http://bats.bios.edu).

b. Plankton community composition

In this study, plankton community composition is defined as the abundance of zooplankton, radiolaria, dinoflagellates, diatoms, the *Prochlorococcus* and *Synechococcus* cyanobacteria, and autotrophic pico- and nano-eukaryote organism groups. *Prochlorococcus* abundance peaked ($>10^5$ cell mL^{-1}) in November and subsequently decreased to ~4×10^4 cell mL^{-1} during January and March (Fig. 1). In contrast to *Prochlorococcus* abundance, cell concentrations of *Synechococcus* are highest during January and March. Phototrophic bacterial cell abundances reported here are consistent with the typical seasonal pattern at the BATS site (DuRand *et al.,* 2001).
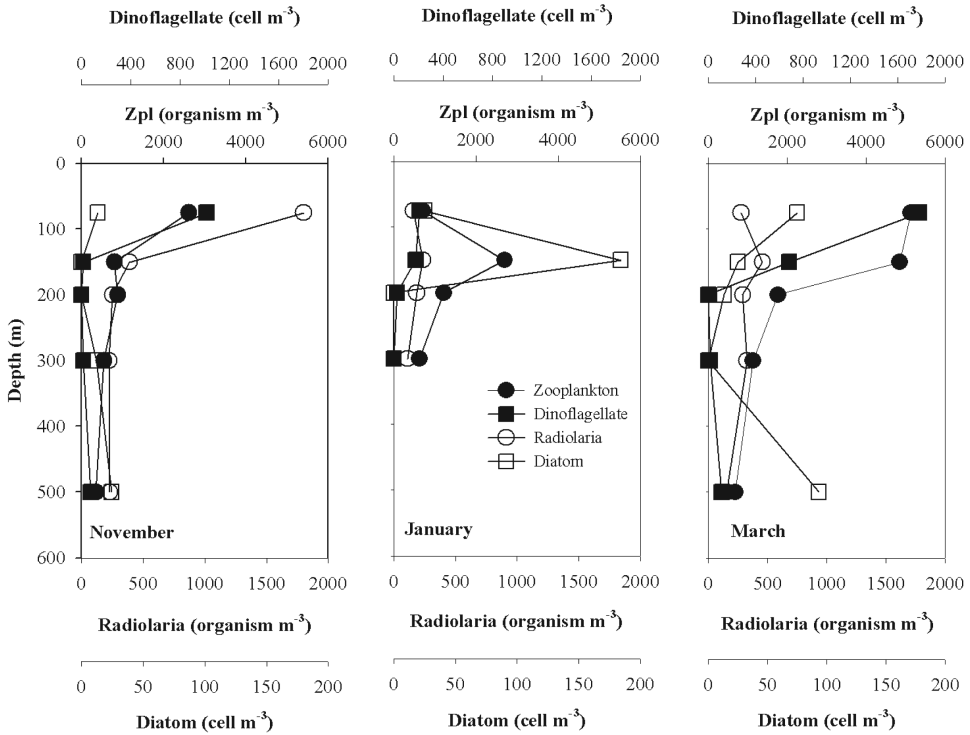
Figure 2. Profiles (0–500 m) of zooplankton, radiolaria, dinoflagellate, and diatom abundance at the
   BATS site during November 2006, January 2007 and March 2007.

The abundance of autotrophic pico-eukaryotes increased during the winter-spring months and was greatest in March, when cell concentrations reached ~1,600 cell mL^{-1} (Fig. 1). In contrast, autotrophic nano-eukaryote cell concentrations reached a maximum (~1,200 cell mL^{-1}) in November. During November, concentrations of nano-eukaryotes at most depths were greater than those of the pico-eukaryotes, a pattern not observed during the winter-spring months.

At most depths, autotrophic *Prochlorococcus, Synechococcus,* pico- and nano-eukaryote abundances during each cruise were similar to seasonally averaged data from 1991–1994 and 2001–present. In March 2007, however, *Synechococcus* and nano-eukaryote abundances were ~two-fold greater than the upper 95% confidence interval and significantly greater than their respective seasonal averages (Lomas, unpub. data).

Total abundance (cell m^{-3}) of zooplankton, radiolaria, dinoflagellate and diatoms from 75–300 m or 500 m are plotted for November, January, and March (Fig. 2). At each depth, the abundance of each organism on every screen (53, 70 and 100-μm) was combined to obtain a total abundance per depth. The greatest radiolaria concentration (~1,800 organism m^{-3}) was during November. The maximum diatom cell concentration (~190 cell m^{-3}) occurred

in January, and dinoflagellate ($\sim$1,800 cell m^{-3}) and zooplankton ($\sim$5,000 organism m^{-3}) abundances peaked during March.

In the analysis that follows, depth-integrated abundances of each organism are compared to ^{234}Th and POC particle size distributions and particle fluxes. The maximum integrated abundances of *Prochlorococcus* (10,000 cell cm^{-2}) and nano-eukaryotes (100 cell cm^{-2}) occurred in November, while the abundances of *Synechococcus* and pico-eukaryotes decreased from May to November and then increased to their peak concentrations (6,000 cell cm^{-2} and 200 cell cm^{-2}, respectively) in March.

c. Size fractionated particulate (10–100 μm) ^{234}Th, OC and POC/^{234}Th ratios

Size fractionated particulate ^{234}Th (^{234}Th$_p$) activities and POC concentrations range between 0.0007 $\pm$ 0.0001 and 0.038 $\pm$ 0.002 dpm L^{-1}, and 0.00021 $\pm$ 0.00001 to 0.135 $\pm$ 0.006 μmol C L^{-1}, respectively (Fig. 3). Although POC was not sampled on 1–10 μm particles, ^{234}Th activities on this size fraction comprise the greatest portion of total ^{234}Th$_p$ during all four months and indicate the prevalence of this particle size class (Brew, 2008).

In all months sampled, the majority of ^{234}Th$_p$ activities decreased or remained constant with depth (Fig. 3). In addition, the majority of the particle size fractionated POC concentrations decreased with depth (Fig. 3), consistent with organism utilization of OC with depth (Suess, 1980).

Large particle, size fractionated (10, 20, 53, 70, 100-μm Nitex) POC/^{234}Th ratios range between 0.28 $\pm$ 0.03 and 24.19 $\pm$ 3.05 μmol dpm^{-1} (Fig. 3). Ratios in most size fractions tend to remain constant with depth during May and November, while a slight decrease with depth is observed during January and March (Fig. 3). As indicated by the January and March ^{234}Th$_p$ activity and POC concentration profiles, in most size classes POC concentration decreases while ^{234}Th$_p$ activity remains nearly constant during these months (Fig. 3).

During all months, large particle, size fractionated POC/^{234}Th ratios were essentially independent of particle size (10–100 μm; Fig. 4). Nearly invariant POC/^{234}Th ratios on the >1-μm and >70-μm size particle at the BATS site have previously been observed (unpub. data within Buesseler *et al.,* 2006). In addition, within their respective analytical uncertainties, there is little difference in average POC/^{234}Th ratios collected during May, November, and January and, in March, the average POC/^{234}Th ratio is slightly higher. Overall during these sampling periods, average POC/^{234}Th ratios range from $\sim$3–4 μmol dpm^{-1} (Fig. 4).

The fractions of total particulate ^{234}Th (X_i^{Th}) and OC (X_i^{POC}) across the large particle (10–100 μm) size spectrum are plotted in Figure 5. In more than half of the 19 distributions, POC and ^{234}Th distribute in a bi-modal fashion with the highest fraction of OC and ^{234}Th in the 10 and 20-μm size classes.

Profiles (150–300 m) of sediment trap POC/^{234}Th ratios exhibit little change with depth in May and November, whereas trap POC/^{234}Th ratios decrease with depth during January and March (Fig. 6). Depth averaged trap POC/^{234}Th ratios in November (5.75 $\pm$ 0.80 μmol dpm^{-1}), January (5.00 $\pm$ 0.61 μmol dpm^{-1}), and March (5.41 $\pm$ 0.64 μmol dpm^{-1}) are identical within the reported uncertainties and, in May, the average ratio
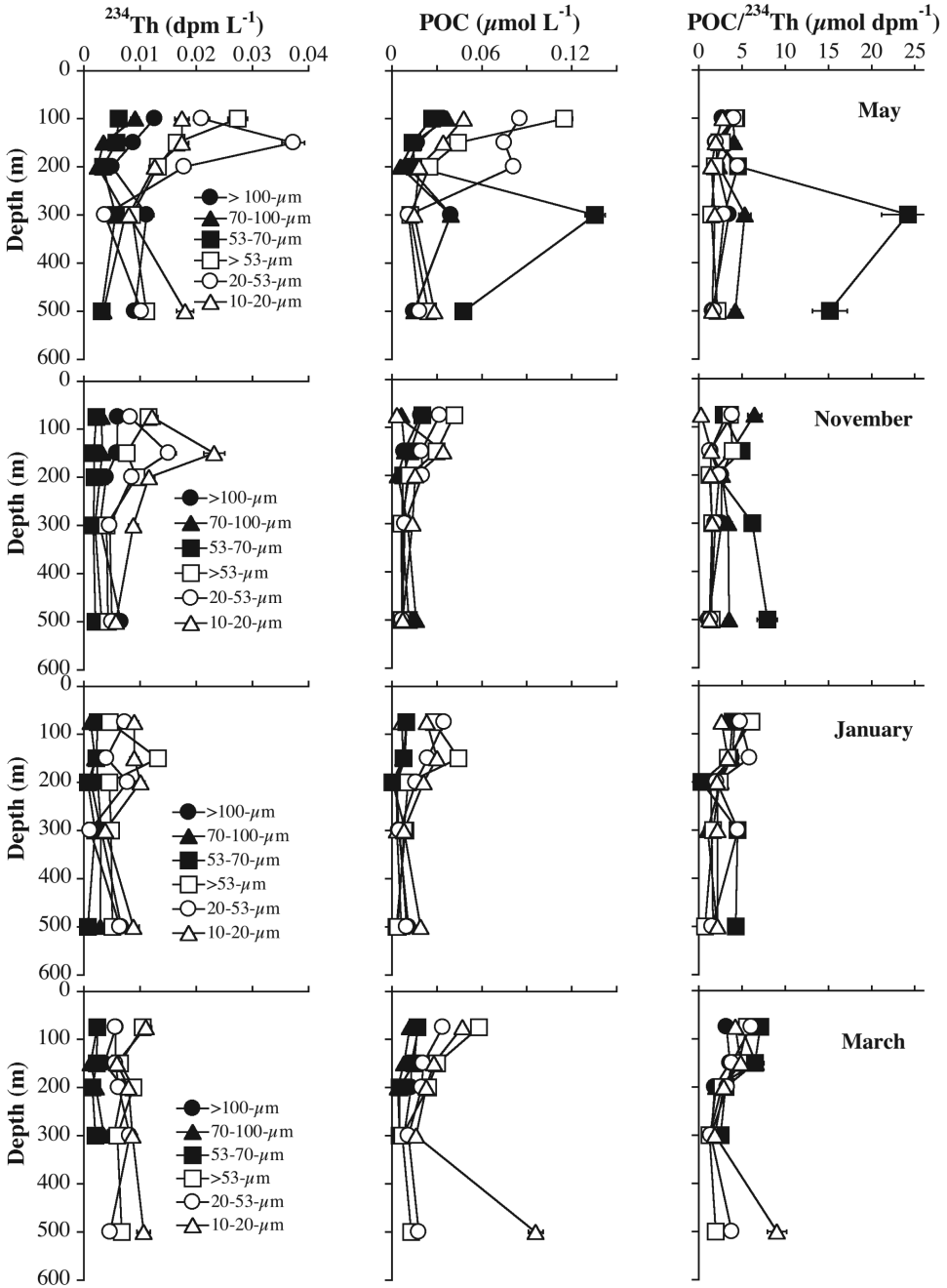
Figure 3. Profiles (0–500 m) of large particle (10, 20, 53, 70, 100-μm) ^{234}Th activities, POC concentrations, and POC/^{234}Th ratios at the BATS site.
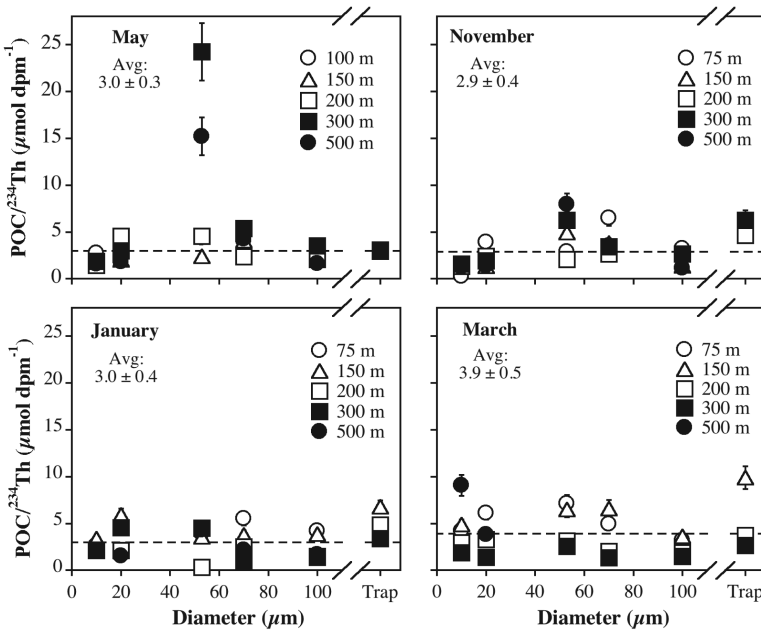
Figure 4. Large particle (10, 20, 53, 70, 100-μm) and sediment trap POC/^{234}Th ratios at the BATS site.

$(2.98 \pm 0.68\ \mu\text{mol dpm}^{-1})$ is only slightly lower (Fig. 4). The measured trap POC/^{234}Th ratios are of similar magnitude to the few previous data from the BATS site (Buesseler *et al.*, unpub. 1993–1995 data referenced in Buesseler *et al.*, 2006), including the more recent values of 3.7–6.7 μmol dpm^{-1} reported by Maiti *et al.* (2009). These values are comparable with trap ratios of ~1–5 μmol dpm^{-1} reported in other oligotrophic regions, such as the equatorial Pacific (Buesseler *et al.*, 1995), Hawaiian Ocean Time-series (HOT) site (Benitez-Nelson *et al.*, 2001) and the Mediterranean (Lepore *et al.*, 2009; Schmidt *et al.*, 2002).

d. ^{234}Th/^{238}U disequilibria and ^{234}Th fluxes

For all cruises, total ^{234}Th activities determined at most depths from duplicate *in-situ* pump casts agree within their analytical errors; similarly, at most depths replicate SV casts agree within the uncertainty of the measurements. For the majority of samples measured during May, January, and March, there is close agreement between ^{234}Th activities determined using the SV and pump methods (Fig. 6). In addition, deep water (500 m) ^{234}Th/^{238}U activity ratios are, with the exceptions noted below, within the uncertainties close to 1, indicating ^{234}Th/^{238}U secular equilibrium at depth during these months. At 5 m depth in May, an apparent ^{234}Th deficit for the *in-situ* pump samples is suspected to be due to a failed flow meter on the pump. As a result, pump ^{234}Th fluxes in May are calculated excluding ^{234}Th activity data from this depth. Similarly, in November, we suspect an
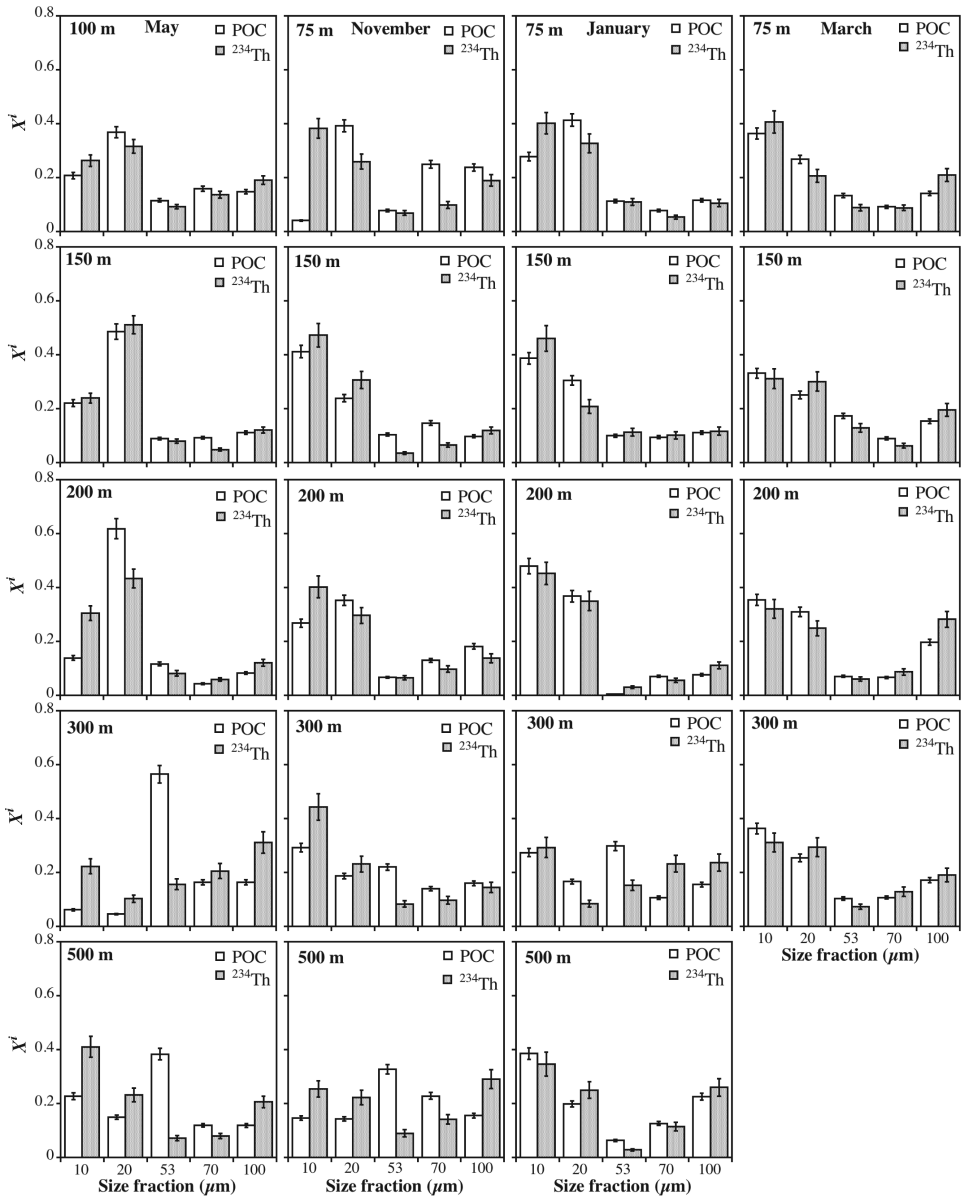
Figure 5. Fractional distributions of particulate ^{234}Th and OC across the large particle size spectrum (10–100-μm) at the BATS site from 75–500 m.

in-situ pump flow meter malfunction may explain the relatively low dissolved ^{234}Th activities compared to the SV ^{234}Th data, particularly at the surface and at 500 m depth. As a result, pump ^{234}Th fluxes in November are not included in this study.
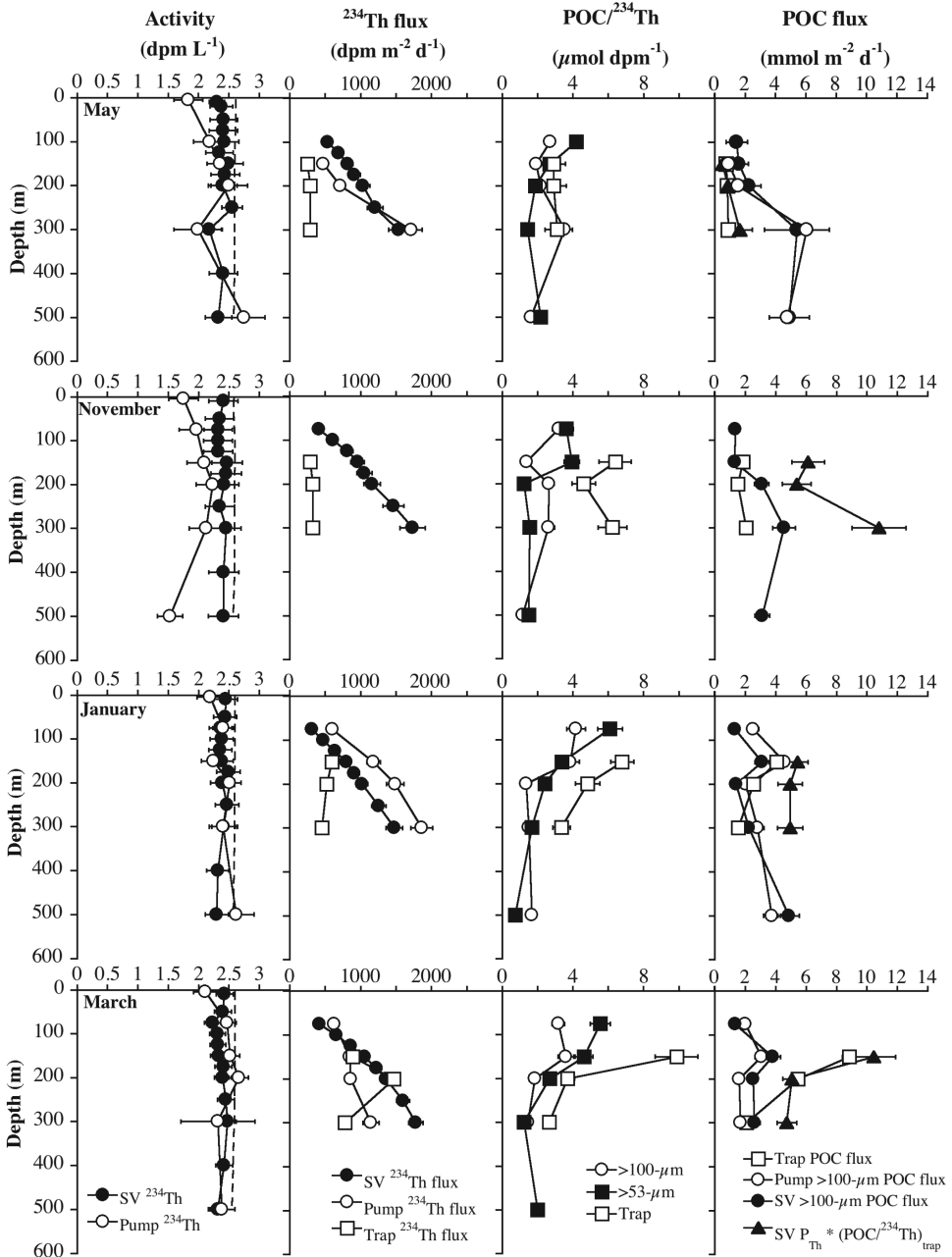
Figure 6. Profiles of total ^{234}Th and ^{238}U activities (dashed line), ^{234}Th fluxes determined using water column sampling devices and sediment traps, POC/^{234}Th ratios on large (100-μm) particle and sediment trap material, and ^{234}Th-derived and sediment trap POC fluxes at the BATS site.

Assuming steady-state and neglecting the transport of ^{234}Th due to diffusion and advection, the flux of ^{234}Th on sinking particles (P_{Th}, dpm m^{-2} d^{-1}) over a prescribed depth interval, $0 - z$ (m) can be calculated using the following relationship,

$$P_{Th} = \lambda \int_0^z (A_U - A_{Th})dz \qquad (1)$$

where, A_U and A_{Th} are the activities (dpm L^{-1}) of ^{238}U and total ^{234}Th, respectively, and λ is the decay constant of ^{234}Th (0.028 d^{-1}).

Water column ^{234}Th fluxes were calculated using Eq. (1) from depth-integrated ^{234}Th deficits obtained using *in-situ* pump and SV methods (Fig. 6). There is no consistent temporal trend, although during all months, *in-situ* pump and SV ^{234}Th fluxes increase with depth (Fig. 6). Trap ^{234}Th fluxes increase temporally from May through March but do not exhibit a consistent trend with depth (Fig. 6). Also, the relative agreement between water column and sediment trap ^{234}Th fluxes varies over the months sampled. In May and November, water column ^{234}Th fluxes are ~two to ~ten-fold greater than trap ^{234}Th fluxes at all depths. A closer agreement between water column and trap ^{234}Th fluxes exists in January and March, (Fig. 6) and fluxes calculated during these months agree to within a factor of ~2–4.

Trap ^{234}Th fluxes in May (~250–300 dpm m^{-2} d^{-1}) are comparable to those reported during May 1992 at the BATS site (Buesseler *et al.,* 1994). The ^{234}Th fluxes reported here are also similar in both magnitude and profile to those recently reported by Buesseler *et al.* (2008) for cyclonic eddies in the Sargasso Sea. Buesseler *et al.* (2008) reported ^{234}Th fluxes at 100 m of ~500 dpm m^{-2} d^{-1} that increased to ~1500 dpm m^{-2} d^{-1} by 300 m. Also, Sweeney *et al.* (2003) reported 30 upper ocean ^{234}Th fluxes determined monthly over three years, with values ranging from ~0–2300 dpm m^{-2} d^{-1} and averaging ~500 dpm m^{-2} d^{-1} over the duration of the study. Overall, ^{234}Th fluxes reported in this study (~250–1500 dpm m^{-2} d^{-1} using traps and ~250–1800 dpm m^{-2} d^{-1} using small-volume and large volume pump methods; Fig. 6) are well within the range of values reported for these independent studies.

In a recent study at the BATS site, Maiti *et al.* (2009) reported steady-state and non-steady-state ^{234}Th fluxes that varied at this location by a factor of ~2–5. Specifically, these authors reported one deployment consisting of five measurements over nine days, and another deployment of three measurements over five days. In both cases, steady-state and non-steady-state models used to calculate fluxes for the five-day deployment indicate a 50% difference in ^{234}Th flux, which is consistent with the variability between traps and SV data presented in this paper. For the three-day deployment, results indicate a larger, ~five-fold, difference between steady-state and non-steady-state fluxes, however the range of ^{234}Th fluxes reported by Maiti *et al.* (2009) using steady-state and non-steady-state models are also in reasonable agreement with those reported here (Fig. 6). Maiti *et al.,* (2009) suggest that advective or diffusive transport of ^{234}Th may result in large differences

between ^{234}Th fluxes determined using steady-state and non steady-state models. In the present study, time-series ^{234}Th measurements were not made and therefore steady-state conditions must be assumed. In addition, the sampling scheme did not allow for the determination of advective and diffusive ^{234}Th transport and so these fluxes are assumed to be small relative to the downward particle export.

e. POC export

From April 2006 through March 2007, sediment trap POC export at 150 m ranged from 0.75 ± 0.04 to 8.83 ± 0.44 mmol C m^{-2} d^{-1}, with enhanced export between January and April 2007 (Fig. 1; http://bats.bios.edu). The lowest and highest export events occurred in May 2006 and March 2007, respectively. Similar to the trend in primary production, trap POC fluxes at 150 m during January (4.06 ± 0.02 mmol C m^{-2} d^{-1}), and March (8.83 ± 0.44 mmol C m^{-2} d^{-1}) are a factor of ~two or more greater than fluxes in May (0.75 ± 0.04 mmol C m^{-2} d^{-1}) and November (1.86 ± 0.09 mmol C m^{-2} d^{-1}). In May, November and January, trap POC data are consistent with seasonally averaged data from 1991–present. In March at 150 and 200 m, however, trap POC data are greater than the long-term seasonal mean by more than a factor of two (data available at http://bats.bios.edu).

Assuming steady-state conditions and that the advective and diffusive transport of ^{234}Th is negligible, the magnitude of POC export (P_{POC}, mmol C m^{-2} d^{-1}) was calculated with the following equation:

$$P_{POC} = \frac{C_{POC}}{A_{Th}^{P}} * P_{Th} \tag{2}$$

where, C_{POC} and A_{Th}^{P} are the concentration of POC (mmol C L^{-1}) and the activity of ^{234}Th (dpm L^{-1}) in sinking particles, respectively, and P_{Th} is the export flux of ^{234}Th on particles (dpm m^{-2} d^{-1}). Note that a key assumption of using the ^{234}Th-normalization method to calculate POC export is that POC and ^{234}Th are removed from the water column on the same particles at the same rate (Moran *et al.,* 2003; Buesseler *et al.,* 2006).

Using Eq. (2), ^{234}Th-derived POC export at 150 m was calculated with water column ^{234}Th fluxes and the POC/^{234}Th ratio of >100-μm filtered particles. During the four months sampled, ^{234}Th-POC export at 150 m ranged from 1.32 ± 0.19 to 3.81 ± 0.52 mmol m^{-2} d^{-1} using SV ^{234}Th fluxes, and 3.07 ± 0.43 to 4.57 ± 0.70 mmol m^{-2} d^{-1} using *in-situ* pump ^{234}Th fluxes (Fig. 6). Consistent with the trend in sediment trap POC export, the SV method indicates lower POC export during May and November and increased export during January and March at 150 m.

The relative agreement between trap and ^{234}Th-estimated POC export varied throughout the months sampled. In May, trap export at 150 m is less than half of the water column estimates. In March, trap export at this depth is greater than ^{234}Th-POC export by a factor of ~2–3. In contrast, during November and January trap and ^{234}Th-derived export agree to within a factor of ~2.
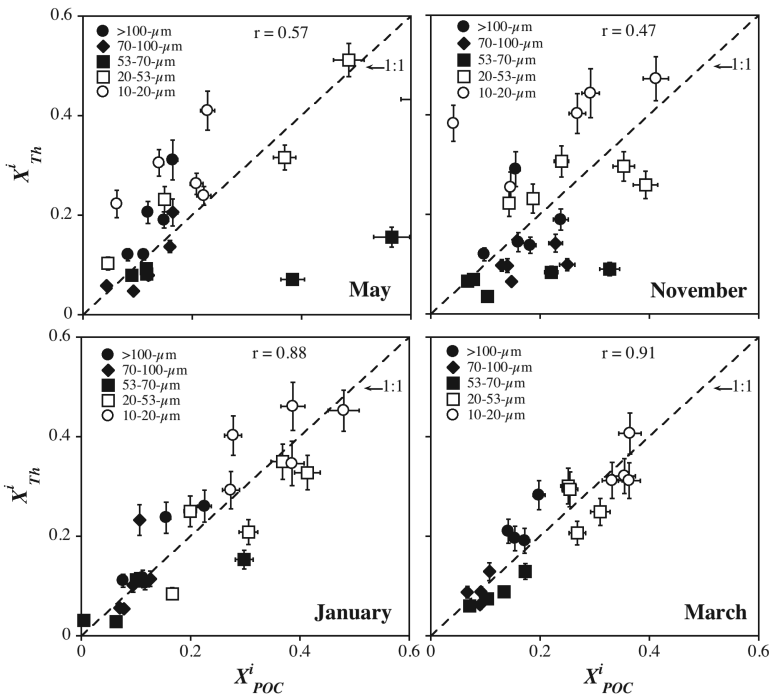
Figure 7. The fractional distribution of ^{234}Th (X_i^{Th}) plotted against the fractional distribution of OC (X_i^{POC}) across the large particle (10–100-μm) size spectrum from 75–500 m. All correlations are statistically significant (P-value $<$ 0.05) and correlation coefficients (r) are shown for each sample month.

4. Discussion

a. Plankton community composition and particle size distributions of OC and ^{234}Th

The degree of correlation between the distribution of OC and ^{234}Th in large, rapidly sinking, particles provides information on the assumption that ^{234}Th and OC are removed from the water column on the same particles (Smith *et al.*, 2006). For each sampling period, the relationship between the OC and ^{234}Th particle size distributions (Fig. 5) was determined from correlation of the fraction of total particulate ^{234}Th measured in size class i (X_i^{Th}, defined here as measured in 10, 20, 53, 70 and 100-μm particles) and the fraction of total POC in size class i (X_i^{POC}) at all depths sampled (Fig. 7). During all months, $X_i^{Th} - X_i^{POC}$ correlations are statistically significant (P-values $<$ 0.05) and there is a greater correlation between the large particle size distributions during January (r = 0.88) and March (r = 0.91) than in May (r = 0.57) and November (r = 0.47) (Fig. 7). These results suggest a tighter coupling between particulate ^{234}Th and OC at the BATS site during the winter-spring bloom period of enhanced primary and export production. Furthermore, whereas POC/^{234}Th ratios are essentially independent of particle size and average ratios are similar between months (Fig. 4), the correlation between the fractional distributions of ^{234}Th and

OC in large particles sampled evidently increases with seasonal increases in primary production and export (Fig. 7).

During each month, the abundance of each organism group enumerated (zooplankton, radiolaria, dinoflagellates, diatoms, the *Prochlorococcus* and *Synechococcus* cyanobacteria, and autotrophic pico- and nano-eukaryotes) was trapezoidally depth-integrated to the maximum sample depth. Correlations of the $X_i^{Th} - X_i^{POC}$ correlation coefficients (r) against each of the integrated organism abundances were determined with a 95% confidence level. The depths included in the $X_i^{Th} - X_i^{POC}$ correlation were adjusted to maintain consistency with the organism integration depths. Because zooplankton, radiolaria, dinoflagellate, and diatom count data were only gathered during November, January and March, correlations using these organism groups include 3 points and are not statistically significant (P-values > 0.05). In contrast, the integrated pico-eukaryote and *Synechococcus* abundances each exhibit a strong (r = 0.97 and 0.85, respectively) positive association with the $X_i^{Th} - X_i^{POC}$ correlation; however, only the pico-eukaryote relationship is statistically significant (P-value < 0.05) (Fig. 8).

While pico-eukaryotes are by definition <3 μm, their depth-integrated abundance is significantly correlated with the observed convergence of OC and [234]Th distributions determined in large particles (Fig. 8). In addition, eukaryotic species are frequently the dominant component of the BATS winter-spring bloom (Haidar and Thierstein, 2001; Lomas and Bates, 2004) and, during the winter-spring bloom period in January and March 2007, at most depths there is a greater than two-fold increase in autotrophic pico-eukaryote cell abundance as compared to concentrations in May and November (Fig. 1). Thus, if the rate of particle aggregation increased during January and March 2007, then the contribution of small cells (including autotrophic pico-eukaryotes) to the downward sinking flux of POC may also have increased.

b. *Plankton community composition and particle export of OC and [234]Th*

In addition to examining the relationship between plankton abundance and particle size distributions of OC and [234]Th (Fig. 8), an objective of this study was to evaluate the correlation between plankton community composition and particle export of OC and [234]Th. As indicated in Figure 9, there are seasonal changes in the depth-integrated abundance of the measured plankton taxonomic groups as well as the particle export flux at 150 m determined using sediment trap, SV, and *in-situ* pump methods. To determine the relationship between plankton community and particle export, sediment trap [234]Th and POC fluxes at 150 m were correlated against depth-integrated (0–140 m) plankton abundances (Fig. 10, Table 2). Because of potential methodological uncertainties related to the assumption of steady-state and neglecting advective and diffusive [234]Th transport, water column [234]Th fluxes and [234]Th-derived POC fluxes were not included in this analysis.

There is a positive correlation between sediment trap [234]Th fluxes and integrated abundance of *Synechococcus* (r = 0.94) and pico-eukaryote (r = 0.98). These results suggest that, in addition to increasing the correlation between the large particle OC and
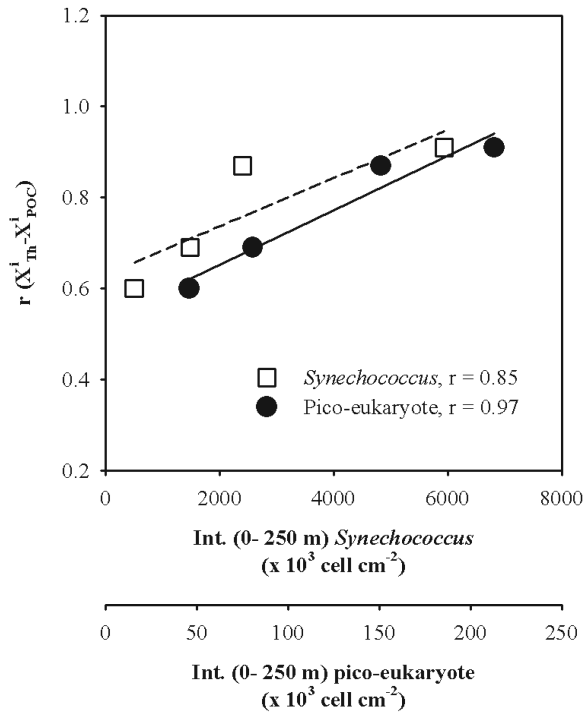
Figure 8. Correlation coefficients describing the relationship between the large particle (10, 20, 53, 70, 100-μm) distributions of ^{234}Th and OC from 75–300 m are plotted against the integrated (0–250 m) abundance of *Synechococcus* and pico-eukaryotes during each month of this study. The pico-eukaryote relationship is statistically significant (P-value < 0.05) and correlation coefficients (r) are shown for each organism.

^{234}Th size distributions, pico-eukaryote abundance may influence the extent to which sinking, ^{234}Th-bound, particles are collected by sediment trap at 150 m. While pico- and nano-plankton have traditionally been thought of as contributing little to export production because of their small size and tight micro-grazer control (e.g., Michaels and Silver, 1988), there is recent evidence to challenge this notion. In particular, pico-plankton may sediment out of the euphotic zone directly through aggregation (Jackson, 1990; 2001; Jackson *et al.,* 2005) or indirectly as fecal pellets if meso-zooplanton consume aggregates containing pico-plankton (Olli and Heiskanen, 1999). More recently, Richardson and Jackson (2007) analyzed the contribution of relative size classes to carbon export from inverse and network analyses and reported that the contribution of pico-plankton was proportional to their high contribution to net primary production.

Although we do not have data on the organisms collected in the sediment trap, evidence at the BATS site suggests there is no statistically significant temporal disconnect between sinking fluxes at 500 and 3200 m, implying an average particulate settling velocity of ~200 m day^{-1} (Conte *et al.,* 2001). Thus, a sediment trap suspended directly below the
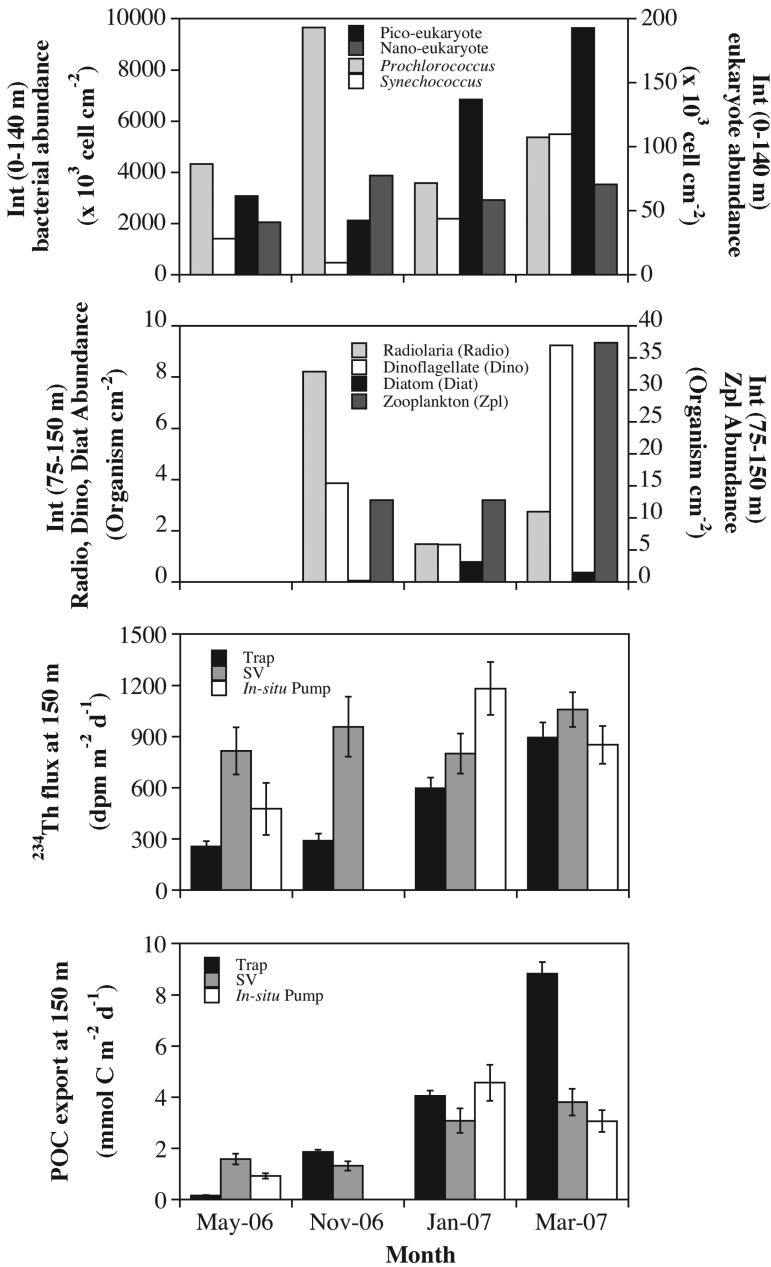
Figure 9. The integrated abundance of autotrophic *Prochlorococcus, Synechococcus,* pico- and nano-eukaryotes, zooplankton, radiolaria, dinoflagellates and diatoms, and water column and sediment trap [234]Th and OC fluxes at 150 m during the months sampled in this study.
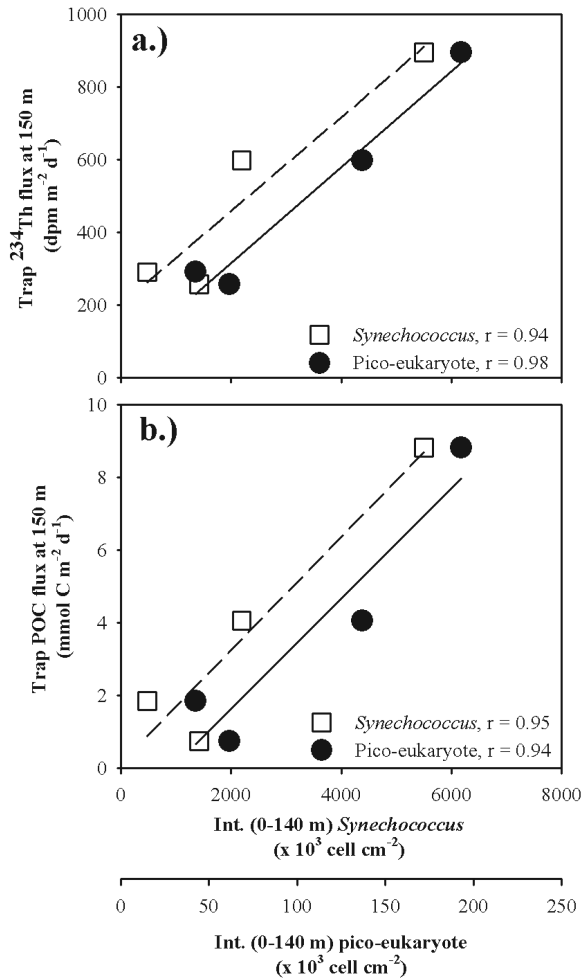
Figure 10. Sediment trap ^{234}Th and OC fluxes at 150 m are plotted against the integrated (0–140 m) abundance of autotrophic *Synechococcus* and pico-eukaryotes during each month of this study. Correlation coefficients (r) are shown for each organism and P-values for each correlation are reported in Table 2.

euphotic zone may collect sinking pico-eukaryotes during the course of a trap deployment (~2–4 days); this would also imply that pico-eukaryotes would have to be sinking as part of aggregates to be sinking at these speeds. *Synechococcus* and pico-eukaryote abundances also show strong positive associations with trap POC export at 150 m (Fig. 10b). However, the P-value for each correlation is ≥0.05 and therefore these relationships are not statistically significant at the 95% confidence level (Table 2).

The correlation between plankton abundance and r($X_i^{Th} - X_i^{POC}$) (Fig. 8) suggests that as primary production and pico-eukaryote abundance increase during the winter-spring

Table 2. Correlation statistics between sediment trap ^{234}Th (dpm m^{-2} d^{-1}) and POC fluxes (mmol C m^{-2} d^{-1}) at 150 m and integrated (0–140 m) plankton abundances (cell cm^{-2})[a]. Correlations are calculated using a 95% confidence level.

Taxonomic group	^{234}Th flux		POC flux	
	r	P-value	r	P-value
Prochlorococcus	0.35	0.66	0.19	0.8
Synechococcus	0.94	0.06	0.95	0.05
Pico-eukaryote	0.98	0.02	0.94	0.06
Nano-eukaryote	0.35	0.66	0.45	0.56
Zooplankton	0.86	0.34	0.95	0.20
Radiolaria	0.77	0.44	0.61	0.58
Dinoflagellate	0.67	0.53	0.81	0.39
Diatom	0.45	0.70	0.24	0.84

[a]Zooplankton, radiolaria, dinoflagellate and diatom abundances were integrated from 0–150 m and measured in organism cm^{-2}. Data for these planktonic groups were not available for May 2006 and therefore the statistical analyses include counts from 3 out of 4 cruises.

months, ^{234}Th may be more tightly coupled to POC-containing particle surfaces. Moreover, the positive correlation between pico-eukaryote abundance and sediment trap ^{234}Th fluxes at 150 m implies that the sinking flux of ^{234}Th-bound particles increases as the abundance of pico-eukaryotes increases. Aggregation rates can increase with increasing cell abundance (Passow, 2002) and the correlations evident in Figure 10 suggest that aggregates of pico-eukaryotic organisms may contribute to the downward sinking flux.

The observations reported for these four cruises can be extrapolated to the longer time-series BATS data. Since the inception of the BATS program, there have been 75 cruises with paired observations of sediment trap POC flux and pico-eukaryote enumeration by flow cytometry. POC flux measurements were conducted by the BATS program, while the pico-eukaryote enumeration was conducted by DuRand *et al.* (2001) from 1991–1994 and by Lomas (unpubl. data) from 2001 to the present. This more extensive data set, while more variable as it covers many years and physical conditions, yields a significant ($P < 0.05$) correlation (Fig. 11). When divided into approximate seasons, summer (July, August, September; JAS) and fall (October, November, December; OND) are at the lower end of the range in observed POC fluxes and pico-eukaryote abundances. Winter (January, February, March; JFM) and spring (April, May, June; AMJ) tend to span the entire observed range. In fact, data for winter alone show a significant correlation between POC flux and pico-eukaryote abundance. Taken together, these observations support the hypothesis of Richardson and Jackson (2007) that pico-plankton may contribute to POC export in oligotrophic systems.

5. Conclusions

Contemporaneous measurements of plankton community composition and particle size fractionated OC and ^{234}Th at the BATS site provide new information on ^{234}Th-OC particle
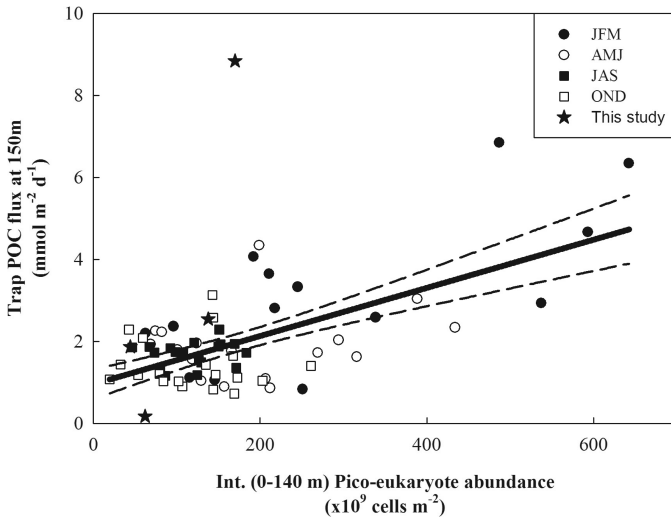
Figure 11. Plot of integrated pico-eukaryote abundance (0–140 m) against POC flux (150 m) for all BATS historical data for which paired data are available. Data are from 1991 to 1994 and 2001 to present. Each datum represents measurements from a separate BATS cruise. Solid black line is the best fit correlation line; dashed lines represent 95% confidence intervals. Data are grouped by month, as noted in the legend.

interactions in association with seasonal changes in primary productivity and upper ocean particle export. These observations suggest that seasonal changes in pico-eukaryote abundance in the water column may affect the interaction between ^{234}Th and OC in large particles and, in turn, the export of large, rapidly sinking particles from this subtropical gyre. In particular, although small in size, changes in the abundance of pico-planktonic organisms may enhance the aggregation of large particles that are exported and captured in upper ocean sediment traps and that ^{234}Th is tracing, an observation that is also supported by recent modeling studies (Richardson and Jackson, 2007).

REFERENCES

Baskaran, M, P. H. Santschi, L. Guo T. S. Bianchi and C. Lambert. 1996. ^{234}Th:^{238}U disequilibria in the Gulf of Mexico: the importance of organic matter and particle concentration. Cont. Shelf. Res., *16,* 353–380.

Benitez-Nelson, C., K. Buesseler, D. Karl and J. Andrews. 2001. A time-series study of particulate matter export in the North Pacific Subtropical Gyre based on ^{234}Th:^{238}U disequilibrium. Deep-Sea Res. I, *48,* 2595–2611.

Boyd, P., J. LaRoche, M. Gall, R. Frew and R. M. L. McKay. 1999. Role of iron, light, and silicate in

controlling algal biomass in subantarctic waters SE of New Zealand. J. Geophys. Res.-Oceans, *104,* 13395–13408.

Brew, H. S. 2008. POC export, ^{234}Th/^{238}U disequilibrium, and plankton community structure in the Sargasso Sea. M.Sc. Thesis, University of Rhode Island.

Brix, H., N. Gruber, D. Karl and N. Bates. 2006. Interannual variability of the relationship between primary, net community and export production in the subtropical gyres. Deep-Sea Res. II, *53,* 698–717.

Buesseler, K. O., J. Andrews, M. Hartman, R. Belastock and F. Chai. 1995. Regional estimates of the export flux of particulate organic carbon derived from thorium-234 during the JGOFS EqPac program. Deep-Sea Res. II, *42,* 777–804.

Buesseler, K. O., A. N. Antia, M. Chen, S. W. Fowler, W. D. Gardner, O. Gustafsson, K. Harada, A. F. Michaels, M. M. Rutgers van der Loeff, M. Sarin, D. K. Steinberg and T. Trull. 2007. An assessment of the use of sediment traps for estimating upper ocean particle fluxes. J. Mar. Res., *65,* 345–426.

Buesseler, K. O., C. Benitez-Nelson, S. B. Moran, A. B. Burd, M. Charette, J. K. Cochran, L. Coppola, N. S. Fisher, S. W. Fowler, W. D. Gardner, L. Guo, Ö. Gustafsson, C. Lamborg, P. Masque, J. C. Miquel, U. Passow, P. H. Santschi, N. Savoye, G. Stewart and T. Trull. 2006. An assessment of particulate organic carbon to thorium-234 ratios in the ocean and their impact on the application of ^{234}Th as a POC flux proxy. Mar. Chem., *100,* 213–233.

Buesseler, K. O., C. Benitez-Nelson, M. Rutgers van der Loeff, J. Andrews, L. Ball, G. Crossin and M. Charette. 2001. An intercomparison of small- and large-volume techniques for thorium 234 in seawater. Mar. Chem., *74,* 15–28.

Buesseler, K. O., J. K. Cochran, M. P. Bacon, H. D. Livingston, S. A. Casso, D. Hirschberg, M. C. Hartman and A. P. Fleer. 1992. Determination of thorium isotopes in seawater by non-destructive and radiochemical procedures. Deep-Sea Res., *39,* 1103–1114.

Buesseler, K. O., C. Lamborg, P. Cai, R. Escoube, R. Johnson, S. E. Pike, P. Masque, D. McGillicuddy and E. Verdeny. 2008. Particle fluxes associated with mesoscale eddies in the Sargasso Sea. Deep-Sea Res. II, *55,* 1426–1444.

Buesseler, K. O., A. F. Michaels, D. A. Seigel and A. H. Knap. 1994. A three dimentional time-dependent approach to calibrating sediment trap fluxes. Global Biogeochem. Cycles, *8,* 179–193.

Charette, M., S. B. Moran, S. Pike and J. Smith. 2001. Investigating the carbon cycle in the Gulf of Maine using the natural tracer thorium-234. J. Geophys. Res., *106,* 11553–11579.

Chen, J., R. Edwards and G. Wasserburg. 1986. ^{238}U, ^{234}U and ^{232}Th in seawater. Earth Planet. Sci. Lett., *80,* 241–245.

Conte, M., N. Ralph and E. Ross. 2001. Seasonal and interannal variability in the deep ocean particle fluxes at the Oceanic Flux Program (OFP)/Bermuda Atlantic Time-series (BATS) site in the western Sargasso Sea near Bermuda. Deep-Sea Res. II, *48,* 1471–1506.

DuRand, M. and R. Olson. 1996. Contributions of phytopankton light scattering and cell concentration changes to diel variations in beam attenuation in the equatorial Pacific from flow-cytometric measurements of pico-, ultra-, and nanoplankton. Deep-Sea Res. II, *43,* 891–906.

DuRand, M., R. Olson and S. Chisholm. 2001. Phytoplankton population dynamics at the Bermuda Atlantic Time-series station in the Sargasso Sea. Deep-Sea Res. II, *48,* 1983–2003.

Fisher, N. S., J.-L. Teyssie, S. Krishnaswami and M. Baskaran. 1987. Accumulation of Th, Pb, U, and Ra in marine phytoplankton and its geochemical significance. Limnol. Oceanogr., *32,* 131–142.

Gunderson, K., K. M. Orcutt, D. A. Purdie, A. F. Michaels and A. H. Knap. 2001. Particulate organic carbon mass distribution at the Bermuda Atlantic Time-series Study (BATS) site. Deep-Sea Res. II, *48,* 1697–1718.

Guo, L., C. Hung, P. Santschi and I. D. Walsh. 2002. ^{234}Th scavenging and its relationship to acid polysaccharide abundance in the Gulf of Mexico. Mar. Chem., *78,* 103–119.

Gustafsson, Ö., P. Andersson, P. Roos, Z. Kukulska, D. Broman, U. Larsson, S. Hajdu and J. Ingri. 2004. Evaluation of the collection efficiency of upper ocean sub-photic-layer sediment traps: a 24-month *in-situ* calibration in the open Baltic Sea using ^{234}Th. Limnol. Oceanogr.: Methods, *2,* 62–74.

Haidar, A. and H. Thierstein. 2001. Coccolithophore dynamics off Bermuda (N. Atlantic). Deep-Sea Res. II, *48,* 1897–1924.

Hung, C.-C., L. Guo, K. A. Roberts and P. Santschi. 2004. Upper ocean carbon flux determined by the ^{234}Th approach and sediment traps using size-fractionated POC and ^{234}Th data from the Gulf of Mexico. Geochem. Jour., *38,* 601–611.

Jackson, G. A. 1990. A model of the formation of marine algal flocs by physical coagulation processes. Deep-Sea Res. I, *37,* 1197–1211.

—— 2001. Effect of coagulation on a model planktonic food web. Deep-Sea Res. I, *48,* 95–123.

Jackson, G. A., A. M. Waite and P. W. Boyd. 2005. Role of algal aggregation in vertical carbon export during SOIREE and in other low biomass environments. Geophys. Res. Lett., *32,* doi:10.1029/2005GL023180.

Kawakami, H. and M. C. Honda. 2007. Time-series observation of POC fluxes estimated from ^{234}Th in the northwestern North Pacific. Deep-Sea Res. I, *54,* 1070–1090.

Lepore, K., S. B. Moran, A. Burd, G. A. Jackson, J. N. Smith, R. P. Kelly, H. Kaberi, S. Stavrakakis and G. Assimakopoulou. 2009. Sediment trap and *in-situ* pump size-fractionated POC/Th-234 ratios in the Mediterranean Sea and Northwest Atlantic: Implications for POC export. Deep-Sea Res. I, *56,* 599–613.

Lohrenz, S. E., G. A. Knauer, V. L. Asper, M. Tuel, A. F. Michaels and A. H. Knap. 1992. Seasonal variability in primary production and particle-flux in the Northwestern Sargasso Sea—United-States JGOFS Bermuda Atlantic Time-Series Study. Deep-Sea Res., *39,* 1373–1391.

Lomas, M. W. and N. R. Bates. 2004. Potential controls on interannual partitioning of organic carbon during the winter/spring phytoplankton bloom at the Bermuda Atlantic Time-series Study (BATS) site. Deep-Sea Res. I, *51,* 1619–1636.

Lomas, M. W., N. L. Roberts, F. Lipschultz, J. Krause, D. M. Nelson and N. R. Bates. 2009. Biogeochemical responses to late-winter storms in the Sargasso Sea. IV. Rapid succession of major phytoplankton groups Deep-Sea Res. I, *56,* 892–908.

Maiti, K., C. Benitez-Nelson, M. W. Lomas and J. Krause. 2009. Biogeochemical responses to late-winter storms in the Sargasso Sea III. Comparison of export production by ^{234}Th and sediment traps. Deep-Sea Res. I, *56,* 875–891.

Michaels, A. and A. Knap. 1996. Overview of the U.S. JGOFS Bermuda Atlantic Time-series Study and the Hydrostation S program. Deep-Sea Res. II, *43,* 157–198.

Michaels, A., A. Knap, R. Dow, J. Gundersen, R. Johnson, J. Sorensen, A. Close, G. Knauer, S. Lohrenz, V. Asper, M. Tuel and R. Bidigare. 1994. Seasonal patterns of ocean biogeochemistry at the U.S. JGOFS Bermuda Atlantic Time-series study site. Deep-Sea Res., *41,* 1013–1038.

Michaels, A. F. and M. W. Silver. 1988. Primary production, sinking fluxes, and the microbial food web. Deep-Sea Res., *35,* 473–490.

Moran, S. B., S. E. Weinstein, H. N. Edmonds, J. N. Smith, R. P. Kelly, M. E. Q. Pilson and W. G. Harrison. 2003. Does ^{234}Th/^{238}U disequilibrium provide an accurate record of particulate organic carbon export flux from the upper ocean? Limnol. Oceanogr. *48,* 1018–1029.

Olli, K. and A.-S. Heiskanen. 1999. Seasonal stages of phytoplankton community structure and sinking loss in the Gulf of Riga. J. Mar. Syst., *23,* 165–184.

Olli, K., C. W. Riser, P. Wassmann, T. Ratkova, E. Arashkevich and A. Pasternak. 2002. Seasonal

variation in vertical flux of biogenic matter in the marginal ice zone and central Barents Sea. J. Mar. Syst., *38,* 189–204.

Passow, U. 2002. Transparent exopolymer particles (TEP) in aquatic environments. Prog. Oceanogr., *55,* 287–333.

Pike, S. M. and S. B. Moran. 1997. Use of Poretics 0.7 μm glass fiber filters for determination of particulate organic carbon and nitrogen in aquatic systems. Mar. Chem., *57,* 355–360.

Quigley, M., P. H. Santschi, C.-C. Hung, L. Gao and B. D. Honeyman. 2002. Importance of acid polysaccharides for Th-234 complexation to marine organic matter. Limnol. Oceanogr., *47,* 367–377.

Richardson, T. and G. Jackson. 2007. Small phytoplankton and carbon export from the surface ocean. Science, *315,* 838–840.

Santschi, P. H., C.-C. Hung, G. Schultz, N. Alvarado-Quiroz, L. Guo, J. Pinckney and I. D. Walsh. 2003. Control of acid polysaccharide production and ^{234}Th and POC export fluxes by marine organisms. Geophys. Res. Lett., *30,* 1044.

Schmidt, S., V. Andersen, S. Belviso and J.-C. Marty. 2002. Strong seasonality in particle dynamics of north-western Mediterranean surface waters as revealed by ^{234}Th/^{238}Th. Deep-Sea Res., *49,* 1507–1518.

Sieracki, M., P. Verity and D. Stoecker. 1993. Plankton community response to sequential silicate and nitrate depletion during the 1989 North Atlantic spring bloom. Deep-Sea Res. II, *40,* 213–226.

Smith, J., S. B. Moran and E. Speicher. 2006. On the accuracy of upper ocean particulate organic carbon export fluxes estimated from ^{234}Th/^{238}U disequilibrium. Deep-Sea Res. I, *53,* 860–868.

Steinberg, D. K., C. A. Carlson, N. R. Bates, R. J. Johnson, A. F. Michaels and A. H. Knap. 2001. Overview of the US JGOFS Bermuda Atlantic Time-series Study (BATS): a decade-scale look at ocean biology and biogeochemistry. Deep-Sea Res. II, *48,* 1405–1447.

Suess, E. 1980. Particulate organic carbon flux in the oceans surface productivity and oxygen utilization. Nature, *288,* 260–263.

Sweeney, E., D. McGillicuddy and K. Buesseler. 2003. Biogeochemical impacts due to mesoscale eddy activity in the Sargasso Sea as measured at the Bermuda Atlantic Time-series Study (BATS). Deep-Sea Res. II, *50,* 3017–3039.

Wassmann, P. 1998. Retention versus export food chains: processes controlling sinking loss from marine pelagic systems. Hydrobiologia, *363,* 29–57.